

Optimization of the Energy Extraction of a Shallow Geothermal System

Markus Beck, Jozsef Hecht-Méndez, Michael de Paly, Peter Bayer, Philipp Blum, Andreas Zell

Abstract—Geothermal energy use from shallow groundwater systems is attractive for the supply of heat and hot water to buildings. It offers economic and environmental advantages over traditional fossil-fuel based technologies, in particular when large scale systems are well adapted to the always unique hydrogeological conditions. Computer based numerical simulations are used to examine the performance of multiple borehole heat exchangers installed in the ground. This paper demonstrates how evolutionary algorithms can be utilized to configure the elements of a geothermal system in an ideal way, and thus substantially enhance the energy extraction rate in comparison to standardized approaches. Differential evolution (DE), evolution strategies (ES) and particle swarm optimizers (PSO) are combined with a local search approach and compared with respect to their efficiency in the optimization of synthetic, real case oriented and static systems. First results are promising, especially for the PSO and the DE with the local search approach.

I. INTRODUCTION

Geothermal energy is a native and environmentally friendly energy. Contrary to most other renewable energy sources, it is available everywhere, independent of geological setting, weather conditions and time of day. For heating and cooling of private houses and other facilities, especially so-called shallow geothermal energy use is on the rise [1]. Here, mostly vertical boreholes are drilled down to a depth of about 100-400 m, and tubes are installed that act as borehole heat exchangers (BHEs). By circulating a glycol/water mixture in these tubes, conductive heat flow is stimulated and the fluid serves as heat carrier. Such systems are called vertical ground source heat pump (GSHP) systems, which, depending on the required energy demand, operate with one single or multiple BHEs. Ultimately the heat is extracted from the subsurface by connecting the BHE with a heat pump [2]. Typically two BHEs are able to sufficiently supply a single-family house with thermal energy. Hence, the simultaneous operation of multiple BHEs may supply an office building, industrial complex or an entire school [3]. Essential for the efficiency of such a BHE field within a given (hydro)geological environment is the overall

dimensioning of the field, i.e. the number and depth of boreholes, as well as individual and coordinated arrangement of the BHEs [4]. The appropriate design of such BHE fields to fulfill a certain demand for energy is straightforward and is based on standardized procedures. In contrast, the optimal design of BHE fields can be a challenging task with various degrees of freedom. BHEs might influence each other. Thus, the highly nonlinear mutual influence between the BHEs needs to be considered in the ideal geometric arrangement. Moreover, the performance of BHE(field)s heavily depends on the local natural conditions, which include the geological environment, groundwater flow and in some cases even interference with other GSHP systems in the neighborhood [2]. Considering all of these criteria for the design of GSHP systems yields a mathematically complex, high dimensional optimization problem. This problem cannot satisfactorily be solved and optimized with the currently available methods or trial-and-error. Currently BHE fields are customarily planned by means of semi-analytical models, such as EED [9] and EWS [8], which are easy to use with short calculation times. These models rely on simplified conditions such as equal heat extraction rates (loads) of all BHEs and a simple geometric arrangement of the BHEs within the field, such as a square lattice. To consider site-specific hydraulic and thermal conditions and to analyze the underground heat transport processes temporally and spatially, numerical models are more suitable [5]. Although numerical models offer much more potential, computational time can be significant and numerical noise often occurs. This is in particular important when the response of such models is used during an automatic optimization procedure. In related studies on model-based optimal water management, Evolutionary optimization Algorithms (EA) are of increasing interest [6], [7]. These algorithms only require objective function values for the optimization of a given problem, are robust and able to handle numerical noise [10]. In the model-based procedure, the design problem is expressed by an objective function that is iteratively evaluated by the EA. In each iteration, candidate solutions are tested by running the numerical model for each candidate and using its response to calculate the objective function value. This concept seems to be promising for larger GSHP systems as well.

In this study we therefore optimize the energy extraction of a BHE field for a synthetic, but real case oriented test case. Selected EAs are used for optimization and the numerical groundwater transport routine MT3DMS [11] is applied for simulating the thermal effects from different configurations of such BHE fields. The GSHP system operates over a

Markus Beck is with the Center for Bioinformatics Tuebingen (ZBIT), University of Tuebingen, Germany, m.beck@uni-tuebingen.de

Jozsef Hecht-Méndez is with the Center for Applied Geosciences (ZAG), University of Tuebingen, Germany, jozsef.hecht-mendez@uni-tuebingen.de

Michael de Paly is with the Center for Bioinformatics Tuebingen (ZBIT), University of Tuebingen, Germany, michael.depaly@uni-tuebingen.de

Peter Bayer is with the Institute for Environmental Engineering, ETH Zurich, Switzerland, bayer@ifu.baug.ethz.ch

Philipp Blum is with the Center for Applied Geosciences (ZAG), University of Tuebingen, Germany, philipp.blum@uni-tuebingen.de

Andreas Zell is with the Center for Bioinformatics Tuebingen (ZBIT), University of Tuebingen, Germany, andreas.zell@uni-tuebingen.de

defined time span and, as a constraint, resulting groundwater temperatures are not allowed to decrease below a regulative limit [2]. Contrary to available design approaches that drive all BHEs with equal loads and confine possible positions of the BHEs, the technique presented here allows the flexible setting of these parameters. Of major interest is the performance of the selected EAs: Which variants are computationally most efficient, which can find favorable parameters for this special design problem, and how many iterations are needed?

II. METHODS

A. Heat transport model

Heat transport in porous media is governed by two mechanisms: heat conduction and heat advection. Heat conduction is driven by a temperature gradient, while heat advection is the transport of heat due to the moving fluid phase. In the geological porous media of shallow geothermal systems, the moving medium is the groundwater. The governing partial differential equation (PDE) that describes groundwater flow is:

$$\nabla \cdot (k \nabla h) + q = S_s \frac{\partial h}{\partial t}, \quad (1)$$

where k is the hydraulic conductivity, h is the hydraulic head, q represents the water source/sink term, S_s is the specific storage of the porous material and t is the time. In heterogeneous systems like the one modeled in the presented study, k is spatially variable. This is typical in natural systems, where for example zones of gravel or sand can be found, all with specific hydraulic properties. For heat transport in the subsurface the PDE is:

$$\begin{aligned} n\rho_w c_w \frac{\partial T_w}{\partial t} + (1-n)\rho_s c_s \frac{\partial T_s}{\partial t} = \\ = (\nabla \cdot [(\lambda_m + n\rho_w c_w \alpha \nu_a) \nabla T]) - \\ - \nabla \cdot (n\rho_w c_w \nu_a T) + q_h, \end{aligned} \quad (2)$$

where n is the porosity, ρ_c , c_w and ρ_s , c_s are the volumetric heat capacities of the materials, λ_m is the arithmetic mean of the thermal conductivity of the water and the solid phase, α represents the thermal dispersivity and ν_a is the seepage velocity. The last term q_h represents the source and sink term. The BHE represents a heat source or sink in the subsurface that disturbs the ambient temperature of the surrounding material. Conductive heat flow is enforced by temperature gradients, in particular by the installed BHEs. Advective heat transport is induced by the prevailing natural head difference, which represents the hydraulic gradient and is linearly proportional to the groundwater flow velocity. Site-specific, often heterogeneous hydraulic and thermal properties of the underground, and the intensity of natural groundwater flow, always create unique conditions.

Two well-established numerical codes used to solve the groundwater flow (Equation (1)) and heat transport equations (Equation(2)) in porous media are MODFLOW [12]

and MT3DMS [11], respectively. Both routines are based on a finite difference solution procedure, are open source and written in FORTRAN. According to [13], MT3DMS is suitable for heat transport simulations of BHEs under a wide range of conditions. An important technical aspect is that by separation of the two codes, MODFLOW only has to be applied once at the beginning of the optimization to simulate flow. Since different BHE configurations affect heat transport, just MT3DMS has to be further used to test candidate solutions, and thus total simulation time can be kept down.

B. Model Setup (Scenarios)

A hypothetical BHE field scenario with 30 BHEs under steady state conditions (800 days) needs to be optimized. The water-bearing stratum (i.e., aquifer) is represented by a one-layer rectangular finite differences model domain. A grid of $\delta x = \delta y = 2.5$ m (Figure 1) is defined to simulate a field case over an area of 500 m \times 500 m. Each BHE is represented by a single grid cell with assigned energy extraction values between 20 W/m and 100 W/m. These are typical values reported for sand and gravel aquifers, respectively [14].

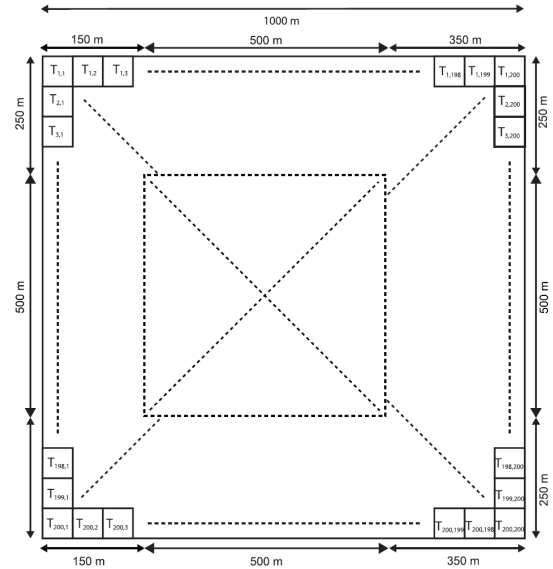


Figure 1. Model domain used in MODFLOW and MT3DMS. The dotted square spans the allocation area for the borehole heat exchangers.

In practice, the diameter of a BHE is around 0.10 m. However, the coarse model resolution of 2.5 m is assumed to deliver a sufficiently good approximation of field conditions, since interference between the BHEs as observed in field cases can be well reproduced. For example, Hecht-Méndez et al. [15] show that assuming a BHE size of 3 m \times 3 m temperature introduces inaccuracies of only < 0.6 K in the vicinity of a BHE. Higher resolution would significantly increase the computational load of the simulation, which is not desirable for this study, as the focus is set on the performance of the optimization algorithms. The proposed

scenario represents an aquifer with three different horizontally distributed hydraulic zones as illustrated in Figure 2. These hydraulic zones represent three different aquifer materials: light grey for gravel, black for sand, and dark grey for silty sand. Along the upper and lower model boundaries, Neumann (no-flow) conditions are set. Using Dirichlet boundary conditions (fixed hydraulic head values at the left and right boundaries), groundwater movement from left to right is simulated. Due to the heterogeneous hydraulic conductivity (k) distribution, the groundwater does not flow along a straight pattern and non-uniform flow pathlines are simulated (Figure 2). Zones of high hydraulic conductivity (or high groundwater flow velocity) focus the flow so that the depicted advective pathlines tend to converge. Equivalent to the hydraulic material parameters, the material-specific thermal parameters (thermal conductivity and volumetric heat capacity) are also heterogeneously distributed.

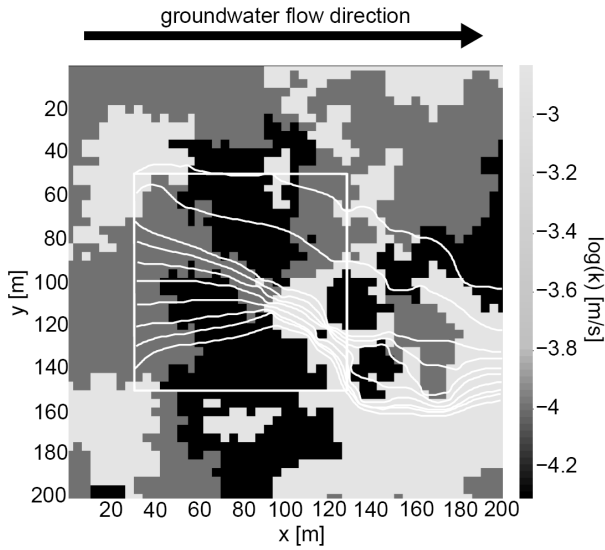


Figure 2. Hydraulic conductivity distributions within the model domain. The white lines illustrate flow paths of 10 water particles that are injected into the model domain. These flow paths were created using MODPATH [16]. The white box represents the available placement area for the 30 BHEs.

C. Objective Function and Constraints

A fixed number of BHEs are to be placed in an area of $250 \text{ m} \times 250 \text{ m}$ in the interior of the model domain as shown in Figure 1. This represents typical field conditions, where the placement of the BHEs is restricted to a building plot. The goal is to find a configuration of BHEs that maximizes the possible energy extraction within a defined simulation time:

$$E_{total}(g) = t \sum_{j=1}^n l_j, \quad (3)$$

where E_{total} is the total extracted energy from the field within the simulation time frame period t for a configuration of BHEs g . n is the number of BHEs in g , and l_j is the thermal power [W] of each BHE j with $j = 1 \dots n$. The

maximum power of each BHE is restricted by a maximum allowed temperature change ΔT_{max} of the underground in the vicinity of the BHE:

$$\Delta T_c \leq \Delta T_{max}, \quad (4)$$

where ΔT_c is the temperature change in cell c caused by the energy extraction of the BHEs. Here ΔT_{max} was set exemplarily to 2.5 K. The influence of a BHE on the aquifer temperature declines with increasing distance. Typical real world applications use a small tolerance area around a given BHE typically between 3 and 10 m [2], and thus the BHE grid cells are not evaluated for this constraint. For the presented study, it is sufficient to evaluate ΔT_c for cells c only in the Moore neighborhoods of all BHE j . The Moore neighborhood comprises the eight cells surrounding the central (BHE) cell on the two-dimensional square lattice.

D. Constraint Handling

BHE loads and positions are subject to a box constraint. The heat extraction values range between 20 W/m and 100 W/m, while the BHEs are allowed to be set in an area of $250 \text{ m} \times 250 \text{ m}$ in the interior of the simulated domain as shown in Figure 1. The temperature constraint (Equation 5) is implemented as a penalty term. If the constraint is violated for a candidate solution, the objective function is significantly reduced:

$$P_c = \begin{cases} 0, & \Delta T_c \leq \Delta T_{max} \\ (\Delta T_c - \Delta T_{max}) & \text{otherwise} \end{cases}, \quad (5)$$

where P_c is the penalty value of cell c . The total penalty value P_{total} for a given configuration of BHEs is calculated by the sum of the penalty values $P_{c(j)}$ of all BHE j . This results in the overall objective (i.e. fitness) function

$$F(g) = E_{total}(g) - P_{total}(g) \cdot \kappa, \quad (6)$$

where κ is a scaling factor for the penalty term. The appropriate choice of κ is crucial for the success of the optimization procedure. Values of κ that are too low may yield optimized solutions with higher fitness values for configurations g of BHEs which violate the temperature constraint. Values of κ that are too high generate a very rugged fitness function which is hard to optimize. An ideal value for κ ensures that in cases of constraint violations the influence of the penalty term always surpasses the influence of the energy function, which can be written for each BHE j as:

$$\kappa \cdot P_{c(j)} > t \cdot l_j, \quad (7)$$

for all cells c in the Moore neighborhood of BHE j . Assuming the worst case with $\Delta T_{max} = 0$ equation (7) results in

$$\kappa > \frac{l_j \cdot t}{\min(\Delta T_c(l_j))} \quad (8)$$

where $\min(\Delta T_c(l_j))$ is the smallest temperature change caused by the load l_j in the Moore neighborhood of BHE j . This relationship enables the determination of a suitable value for κ based on the hydraulic properties of the given scenario prior to the actual optimization procedure.

E. Encoding of individuals

A configuration of a BHE field g with n BHEs can be written as a vector of the BHEs $j = 1, \dots, n$, each defined by a position (x_j, y_j) and a thermal power l_j . This yields an overall vector

$$g = (x_1, x_2, \dots, x_n, y_1, y_2, \dots, y_n, l_1, l_2, \dots, l_n) \quad (9)$$

Within the evolutionary optimization process each candidate solution, i.e. individual i of generation m is assigned a single BHE field-vector $g_i^{(m)}$ as defined above. In the studied optimization problem (x_j, y_j) represent cell coordinates which are integer values while the loads l_j are real valued.

F. A local search approach

In existing designs of BHE fields all BHEs are driven with the same loads. Especially in case of groundwater flow and dominant advective heat transport, such designs do not seem ideal. Unwanted interference between neighboring BHEs can occur, e.g. if one BHE is positioned downwards along the gradient of another one. In such a case, lower loads are favorable for the downgradient BHE in order to comply with the temperature constraint. Similar relationships can be observed for BHEs positioned in areas with different geological properties. As suggested here, a remedy could be to assign different loads to each BHE of the BHE fields. However, using this degree of freedom significantly increases the dimension of the optimization problem.

In the presented study, a hierarchical approach with two separate optimization steps is suggested, one for the geometric design and one for the loads. Each time the EA generates an individual $g_i^{(m)}$ its loads l_1, \dots, l_n are separated from its coordinates and optimized independently with a local search approach under the use of an objective function (Equation (12)) in a separate step. The objective function assigns a single fitness value to every BHE load, depending on the extracted energy of the BHE and the adherence of the temperature constraint. A higher energy extraction of the BHE yields a better fitness value and a violation of the temperature constraint impairs the fitness depending on the extent of the violation. The local search approach runs over five iteration cycles and, since the result can also be a degraded performance of the BHE field, the global fitness for each local search step is calculated. Depending on the fitness the loads will be increased or reduced in the next iteration step. Finally, the load values of the search step with the best global fitness are assigned to the current individual.

Hence the local search never results in reduced global fitness values. In order to achieve maximum energy extraction and concurrently adhere to the temperature constraint each BHE should be driven with loads close to constraint-violating values. The maximum load value l_j^{opt} for a BHE j that does not produce a constraint violation is defined as:

$$l_j^{\text{opt}} = \max(l_j | P_j = 0) \quad (10)$$

where P_j is the sum of the penalty values P_c of all cells c in the Moore neighborhood of BHE j . The objective function for load l_j of BHE j derives from equation (6)

$$F(g) = E_{\text{total}}(g) - P_{\text{total}}(g) \cdot k = \sum_{j=1}^n l_j - k \cdot \sum_{j=1}^n P_j = \sum_{j=1}^n (l_j - k \cdot P_j) \quad (11)$$

and writes

$$F(l_j) = l_j - k \cdot P_j \quad (12)$$

In case of no interaction between the BHEs, l_j^{opt} would be the global optimum of the objective function (12), and according to (11) and (12) the assignment of the load value of each BHE j with l_j^{opt} would be the global optimum of function (6). In reality and in our model setup, limited building ground results in a high spatial closeness of BHEs and mutual influence between individual BHEs is inevitable. In the event of positioning a BHE downstream of another BHE it could be more efficient to drive both BHEs with medium loads than use the first BHE to full capacity and turn down the second one nearly completely. Thus assigning each BHE j with l_j^{opt} will not necessarily lead to the global optimum of (6) and the best solution of the overall optimization problem. Although this approach is not able to find the global optimal individual load values for each BHE in each case, it nevertheless can be used to move the loads closer to l_j^{opt} and to support the EA by avoiding individuals with bad fitness values due to extremely high or low load values.

Equation (12) represents a convex function in a one dimensional search space. Thus local improvement procedures should be an ideal compromise between speed of convergence and efficiency for the detection of the global optimum. We went for the linesearch algorithm because it is easy to implement and excellent for finding global optima of objective functions in one dimension. The number of linesearch iterations was set to five in each enhancement step.

III. OPTIMIZATION ALGORITHMS AND PROCEDURE

A. Algorithms

We used our open source Evolutionary Algorithm framework EvA2, which is a comprehensive optimization system written in Java, with a wide range of evolutionary algorithms, like evolution strategies (ESs), genetic algorithms (GAs), genetic programming (GP), particle swarm optimization (PSO)

and differential evolution (DE) [17]. We applied the following Evolutionary Algorithms on the problem of optimizing a BHE field.

1) Evolution Strategy (ES).

A population of μ parents generates a set of λ children via mutation and recombination operators. A following selection step chooses μ individuals for the next generation from the set of either the offspring, referred to as (μ, λ) -selection ($\mu < \lambda$ must hold), or both the parents and offspring, referred to as $(\mu + \lambda)$ -selection. In this paper we used a $(5, 40) - ES$ with $\frac{1}{5}$ -success rule as mutation operator and one-point crossover with ($p_c = 0.5$) for recombination.

2) Particle Swarm Optimization Algorithm (PSO).

In PSO, a set of individuals is represented by a so-called swarm that is composed of a set of particles $P = \{p_1, p_2, \dots, p_n\}$. At any time step t , p_i has a position \vec{x}_i^t and a velocity \vec{v}_i^t associated with it. A candidate solution of the optimization problem is represented by the position of a particle. For every particle p_i the best solution it has ever reached until time step t is represented by vector \vec{b}_i^t . Further, every particle receives information from its neighborhood $N_i \subseteq P$ while neighborhood relations are commonly represented as a graph $G = \{V, E\}$. The particles' position and velocity are updated by so-called update rules after every time step t . In the presented study we decided on a grid topology and a swarm size of $n = 30$. To update the particles' positions and velocities the constriction mode with $\phi_1 = \phi_2 = 2.05$ is chosen.

3) Differential Evolution (DE).

In DE a population consists of μ individual vectors x_1, \dots, x_μ . A mutation vector ν_j is assigned to every individual vector x_j whereas the calculation of ν_j depends on the chosen mutation mode and a mutation factor F . In the following recombination step a trial vector u_j composed of elements of x_j and ν_j is created. A final selection step calculates the fitness of x_j and u_j and only the vector with the better fitness value will be overtaken in the next generation. For our optimization runs we decided for a DE/current-to-best/1 Differential Evolution with $F = 0.7$ and a cutoff probability $C_r = 0.8$ for the recombination step.

All algorithms were tested with as well as without the local search approach, so the number of tested algorithms rises to six (ES, PSO, DE, LS-ES, LS-PSO, LS-DE). According to equation (8) the scaling factor κ was set to $\kappa = 1250$. To obtain statistically significant results each algorithm run was started 10 times. To keep the overall runtime in an admissible range we limited the number of objective function calls for each algorithm to 75 000. For the same reason, we implemented an additional stop criterion that aborts a test run if no better fitness value was found for 6000 objective function calls. With our parameter configuration, one MT3DMS simulation takes about 3 minutes. Hence one optimization run with 75 000 objective function calls

brings up an overall runtime of 225 000 minutes or 156 days. The calculations were executed on AMD Opteron computer cluster and with a tenfold parallelization of the EAs we were able to reduce the runtime for one optimization run to two weeks.

B. Results

Figure 3 and Table I show the optimization results of the six tested algorithms. For further evaluation of the results we only consider those algorithms that produced valid solutions in terms of the constraints mentioned in II-D.

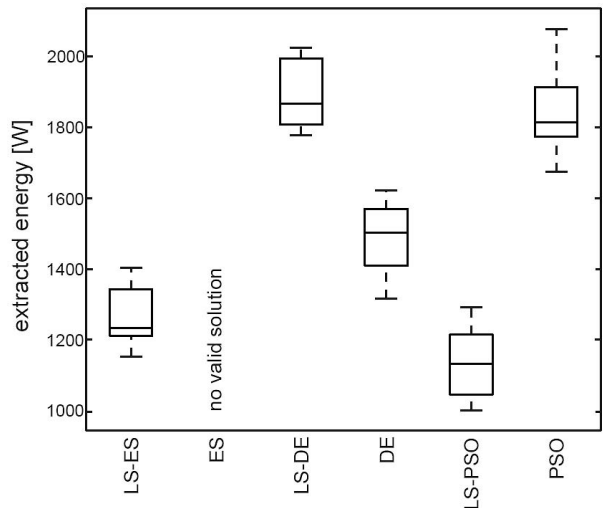


Figure 3. Boxplot of the optimization results. The fitness values are expressed in Watt. Every algorithm was tested ten times. On each box, the central mark is the median, the edges of the box are the 25th and 75th percentiles, the whiskers extend to the most extreme data points not considered outliers.

Table I
SHOWS A COMPARISON OF THE RESULTS. THE VALUES CORRESPOND TO THE EXTRACTED ENERGY OF THE BHE FIELDS IN [W].

Algorithm	Best	Avg.	Std.
DE	1622	1480	112
LS-DE	2024	1887	96
PSO	2077	1853	120
LS-PSO	1291	1139	98
ES	no valid solution	no valid solution	no valid solution
LS-ES	1404	1268	84

LS-DE and PSO outperformed the other algorithms and achieved the best results. ES is not able to achieve valid solutions without the local search approach. Although PSO gave a better peak result than LS-DE, LS-DE attained a slightly better average performance. LS-DE and PSO are the only algorithms that were not stopped before the limit of 75 000 objective function evaluations was reached. The other algorithms were aborted after considerably fewer objective function evaluations according to the stop criterion given in III-A. In comparison, ES, LS-ES and DE showed overly strong convergence behaviour and terminated in local optima very soon. These findings reflect

the extremely multimodal character of the objective function. We suggest that the high selection pressure of the ES is the reason that this algorithm could not detect valid solutions at all. PSO was the only algorithm that achieved significantly better results without the local search approach.

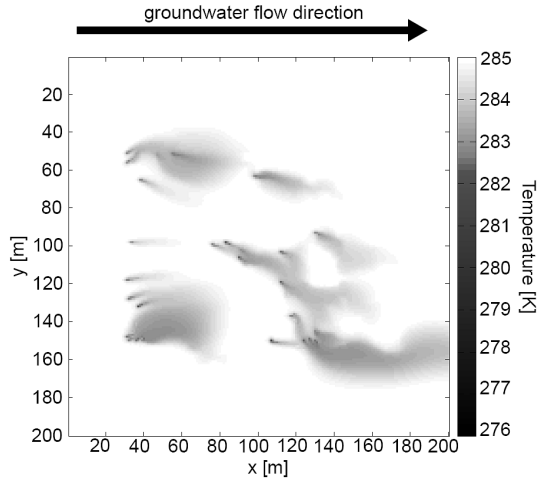


Figure 4. Temperature distribution in the underground of the best BHE setup found by PSO. The overall energy extraction of the BHE field equals the energy extraction of the field illustrated in Fig. 5 but the defined temperature constraint is respected.

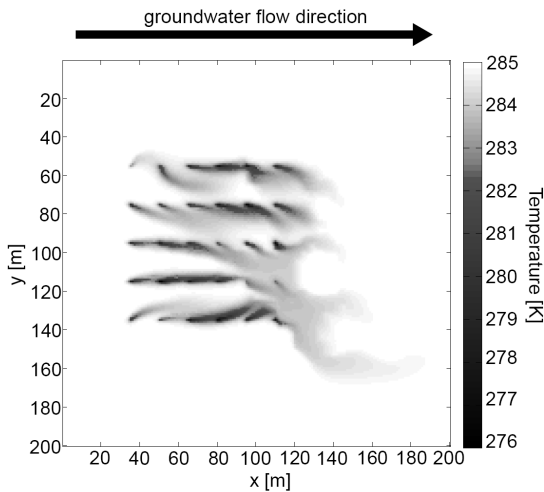


Figure 5. Temperature distribution in the underground with a lattice-like arrangement of 30 BHEs and equal loads (67.5 W/m) for all BHEs. The field is parameterized as described in II-B and the energy extraction of the BHE field equals the energy extraction value of the best BHE field found by PSO (illustrated in Fig. 4). 28 of 30 BHE generate temperature changes in the underground that exceed ΔT_{max} at least in one cell in the Moore neighborhood of the BHE cell.

This effect can be attributed to the external change of the individual vectors by the linesearch algorithm between the creation and the evaluation of the individuals by PSO. Because of this external perturbation, the kinetic energy of the particle swarm remains nearly static and the convergence behaviour of PSO becomes less satisfactory. Figures 4 and

5 compare the temperature distribution in the underground after one MT3DMS simulation run within two BHE fields.

Both BHE fields extract the same amount of energy. Figure 4 presents the best BHE field found by PSO and shows that the temperature constraint is adhered to. The temperature distribution in Figure 5 results from a lattice-like arrangement of 30 BHEs and equal extraction rates for each BHE of 67.5 W/m. The loads of this field are assigned to the mean of the loads of the best BHE field found by PSO. That means the load $l_j^{lattice}$ of a BHE j in the lattice arrangement was set to the extracted energy of the best BHE field found by PSO divided by 30. Using this lattice array and without considering the temperature constrain defined in II-D, the temperature change of the subsurface exceeds ΔT_{max} up to 6.5 K. To achieve an adherence of the temperature to the lattice arrangement, the loads would have to be dimmed to 23 W/m. This means a reduction of the loads by 67% compared to the optimal BHE field found by LS-DE.

IV. CONCLUSION

In this study we presented an application of three EAs (ES, DE, PSO) to the problem of optimizing the energy extraction of a ground source heat pump system with 30 BHEs over a defined time. A minimum temperature constraint, which ensures that the temperature changes of the subsurface by heat extraction remain in reasonable bounds, was defined. We introduced an objective function and a constraint handling strategy, that ensured the adherence to the minimum temperature criterion of the subsurface. Contrary to current design approaches, which drive all BHEs with equal loads and allow only a constricted arrangement for the positions of the 30 BHEs, our optimizers are allowed to set these parameters freely within defined ranges. Furthermore, we introduced a local search procedure for an additional fine adjustment of the individual extraction rates. Each EA was tested with and without the local search approach, so the number of tested algorithms rose to six (ES, LS-ES, DE, LS-DE, PSO, LS-PSO). LS-DE and PSO outperformed the other algorithms and achieved the best results, while the ES was not able to achieve valid results without the local search approach at all. The optimized BHE fields ensure a high energy yield and at the same time ensure reasonable temperature changes of the subsurface within the temperature constraint. Fields designed according to the actual lattice shaped design of BHE fields, where all BHEs are assigned with same energy extraction rates, violated the temperature constraint severely. Without violating the temperature constraint, the lattice shape BHE field could only reach 33% of the energy extraction of the optimized BHE fields.

Attractive prospects for future work are to test further EAs with the given problem and to further evaluate the best EAs found in this study (LS-DE and PSO) in respect to various hydrogeological conditions or advanced real case scenarios.

ACKNOWLEDGMENTS

This work was supported by the Deutsche Bundesstiftung Umwelt (DBU), the Landesstiftung Baden-Württemberg and

the Federal Ministry for Education and Research (BMBF) scholarship program for International Postgraduate Studies in Water Technologies (IPSWaT).

REFERENCES

- [1] A. H. Demirbas, "Global geothermal energy scenario by 2040," *Energy Sources, Part A: Recovery, Utilization, and Environmental Effects*, vol. 30, pp. 1890 – 1895, 2008.
- [2] S. Hähnlein, N. Molina-Giraldo, P. Blum, P. Bayer, and P. Grathwohl, "Ausbreitung von Kältefahnen im Grundwasser bei Erdwärmesonden (Cold plumes in groundwater for ground source heat pump systems)," *Grundwasser*, no. 15(1), 2010.
- [3] A. M. Omer, "Ground-source heat pumps systems and applications," *Renewable and sustainable energy review*, pp. 344–371, 2008.
- [4] S. P. Kavanaugh and K. Rafferty, "Ground Source Heat Pumps - Design of Geothermal Systems for Commercial and Institutional Buildings," *American Society of Heating, Refrigerating and Air-Conditioning Engineers*, 1997.
- [5] T. Schmidt and G. Hellström, "Ground Source Cooling Working Paper on Usable Tools and Methods," EU Commission SAVE Programme and Nordic Energy Research, Tech. Rep., 2005.
- [6] P. Bayer, C. M. Bürger, and M. Finkel, "Computationally efficient stochastic optimization using multiple realizations," *Advances in Water Resources*, no. 31(2), pp. 399 – 417, 2008.
- [7] M. de Paly and A. Zell, "Optimal Irrigation Scheduling with Evolutionary Algorithms," in *Applications of Evolutionary Computing*, vol. 5484/2009. Springer-Verlag Berlin/Heidelberg, April 2009.
- [8] M. Wetter and A. Huber, *Vertical Borehole Heat Exchanger EWS Model*, 1997.
- [9] T. Blomberg, J. Claesson, P. Eskilson, G. Hellström, and B. Sanner, *EED 3.0 Earth Energy Designer*, 2008. [Online]. Available: www.buildingphysics.com
- [10] D. Arnold, *Noisy Optimization with Evolution Strategies (Genetic Algorithms and Evolutionary Computation)*. Springer, 2002.
- [11] C. Zheng and P. Wang, "MT3DMS: A Modular Three-Dimensional Multispecies Transport Model for Simulation of Advection, Dispersion, and Chemical Reactions of Contaminants in Groundwater Systems; Documentation and User's Guide," in *Contract Report SERDP-99-1, U.S. Army Engineer Research and Development*, 1999.
- [12] A. Harbaugh, E. Banta, M. Hill, and M. McDonald, *MODFLOW-2000, the U.S. Geological Survey modular ground water model, user guide to modularization concepts and the ground water flow process*, 2000.
- [13] J. Hecht-Méndez, N. Molina-Giraldo, P. Blum, and P. Bayer, "Evaluating the solute transport model MT3DMS for heat transport simulation of closed shallow geothermal systems," *Ground Water*, in press.
- [14] VDI, "Thermische Nutzung des Untergrundes: Erdgekoppelte Wärmepumpenanlagen, VDI-Richtlinie 4640," 2001.
- [15] J. Hecht-Méndez, N. Molina-Giraldo, P. Blum, and P. Bayer, "Use of MT3DMS for heat transport simulation of shallow geothermal systems." World Geothermal Congress 2010, 2010.
- [16] *MODPATH: User's guide for MODPATH/MODPATH-PLOT, version 3: A particle tracking post-processing package for MODFLOW, the USGS finite-difference ground-water flow model.*, 1994.
- [17] F. Streichert and H. Ulmer, *JavaEvA : a Java based framework for Evolutionary Algorithms*. [Online]. Available: <http://tobias-lib.uni-tuebingen.de/volltexte/2005/1702>